

# Bis(trifluoroaceto) Disulfide (CF<sub>3</sub>C(O)OSSOC(O)CF<sub>3</sub>): A HeI Photoelectron Spectroscopy and Theoretical Study

Xiaoqing Zeng,<sup>†,‡</sup> Maofa Ge,<sup>\*,†</sup> Zheng Sun,<sup>†</sup> and Dianxun Wang<sup>\*,†</sup>

State Key Laboratory for Structural Chemistry of Unstable and Stable Species, Institute of Chemistry, Chinese Academy of Sciences, Beijing, 100080, China, and Graduate School of Chinese Academy of Sciences, Beijing, 100039, China

Received: February 18, 2006; In Final Form: March 14, 2006

Bis(trifluoroaceto) disulfide CF<sub>3</sub>C(O)OSSOC(O)CF<sub>3</sub> was prepared and studied by Raman, photoelectron spectroscopy (PES), and theoretical calculations. This molecule exhibits gauche conformation with both C=O groups cis to the S–S bond; the structure of the OSSO moiety is characterized by dihedral angle  $\delta_{\text{OSSO}} = -95.1^\circ$  due to the sulfur–sulfur lone pair interactions. The contracted S–S bond (1.979 Å) and relatively high rotational barrier (19.29 kcal mol<sup>-1</sup> at the B3LYP/6-31G\* level) of the  $\delta_{\text{OSSO}}$  indicate the partial resonance-induced double bond character in this molecule. After ionization, the ground cationic-radical form of CF<sub>3</sub>C(O)OSSOC(O)CF<sub>3</sub><sup>•+</sup> adopts a trans planar main-atom structure ( $\delta_{\text{OSSO}} = 180^\circ$  and  $\delta_{\text{OCOS}} = 0^\circ$ ) with *C*<sub>2h</sub> symmetry. The S–S bond elongates to 2.054 Å, while the S–O bond shortens from 1.755 Å in neutral form to 1.684 Å in its corresponding cationic-radical form. The adiabatic ionization energy of 9.91 eV was obtained accordingly. The first two HOMOs correspond to the electrons mainly localized on the sulfur 3p lone pair MOs:  $3p\pi \{36a (n^{\text{A}}_{\text{S}})\}^{-1}$  and  $3p\pi^* \{35b (n^{\text{B}}_{\text{S}}, n^{\text{B}}_{\text{O}(\text{C}=\text{O}))}\}^{-1}$ , with an experimental energy separation of 0.16 eV. The first vertical ionization energy is determined to be 10.81 eV.

## Introduction

Compounds with the formula ROSSOR were first synthesized in 1895,<sup>1</sup> but have been generally overlooked until the past few years.<sup>2–4</sup> The simplest molecule of ROSSOR compounds is dihydroxydisulfane HOSSOH, the chainlike isomer of thiosulfurous acid. This molecule has been detected by means of neutralization–reionization mass spectrometry, but the free acid is unstable and hence unknown in the isolated state.<sup>5</sup> The calculations on the seven isomers of H<sub>2</sub>S<sub>2</sub>O<sub>2</sub> predicted that the chainlike isomer is one of the most stable.<sup>6</sup> Later, the relatively stable methyl ester dimethoxydisulfane CH<sub>3</sub>OSSOCH<sub>3</sub> was extensively studied: electronic structure by photoelectron spectroscopy,<sup>7</sup> crystal structure in the solid state with XRD,<sup>8</sup> conformational structure in the gas phase with vibrational spectroscopy (IR and Raman), and the gas electron diffraction (GED) method.<sup>9</sup> The results reveal that this molecule occurs as two different rotational isomers in the gas phase and in the solid state. The molecule is chainlike and asymmetrical in the gas phase with *C*<sub>1</sub> symmetry, while it adopts a slightly distorted *C*<sub>2</sub> symmetry in the crystal. Ab initio MO calculations show the former conformer to be more stable than the latter by 0.96 kcal mol<sup>-1</sup>; a third conformer of *C*<sub>2</sub> symmetry was found by calculations to be the least favorable due to the sterical interactions of the methyl groups.

Recently, many compounds with the OSSO moiety have been extensively investigated by NMR on discussing the existence of M and P enantiomers, the barriers of S–S rotation, as well as isomerization from “unbranched” ROSSOR to “branched” ROS(=S)OR.<sup>10–14</sup> One of the defining and highly unusual

properties of ROSSOR is the exceptionally short S–S bond (1.960(3) Å of CH<sub>3</sub>OSSOCH<sub>3</sub><sup>8</sup>) in contrast to 2.031(3) Å in MeSSMe;<sup>15</sup> it indicates a much higher (ca. 18 kcal mol<sup>-1</sup>) S–S rotational barrier than that of a normal disulfide (ca. 7 kcal mol<sup>-1</sup>). Restricted S–S bond rotation in ROSSOR appears to arise entirely from electronic modulation of the S–S  $\sigma$ -bond. Indeed, the degree of this electronic effect manifests itself through electron-withdrawing elements immediately adjacent to the S–S bond. However, restricted rotation around a single bond is not usually influenced solely through stereoelectronic interactions; other interactions such as the repulsion of S–S, S–O lone pair electrons should also be considered as well in some cases.

Lone pair interactions in unsymmetrical systems, RSSR vs RSOR, were discussed by Snyder et al. in 1977 by means of semiempirical MO calculations.<sup>16</sup> Particular attention was paid to the  $\alpha$ -lone pair interactions, and the study concluded that the two species are predicted to exhibit comparable equilibrium geometries, while the resemblance of the molecular orbital energy levels between two systems is absent. Experimental studies on the S–S lone pair interactions were carried out by Ng et al., when discussing the adiabatic ionization energy (*I*<sub>a</sub>) of CH<sub>3</sub>SSCH<sub>3</sub> with the photoionization mass spectrometric method.<sup>15</sup> The observed first adiabatic ionization energy *I*<sub>a</sub> = 8.18 eV is much lower than the first vertical ionization energy (*I*<sub>v</sub> = 8.98 eV), which is attributed to the low potential rotational barrier of the S–S bond, as well as the S–S lone pair interactions. Calculations also predicted that the cationic-radical form CH<sub>3</sub>SSCH<sub>3</sub><sup>•+</sup> adopts a planar ( $\delta_{\text{CSSC}} = 180^\circ$ ) conformation, while the neutral molecule adopts a gauche conformation with  $\delta_{\text{CSSC}} = 85.1(4)^\circ$ . Similar dramatic changes in geometry after ionization also have been observed in other fluorocarbonyl (di- and tri-) sulfur compounds FC(O)SSCH<sub>3</sub> and FC(O)SSSC(O)F.<sup>17,18</sup>

\* Author to whom correspondence should be addressed. E-mail: gemaofa@iccas.ac.cn.

<sup>†</sup> Institute of Chemistry, Chinese Academy of Sciences.

<sup>‡</sup> Graduate School of Chinese Academy of Sciences.

In the present study, we report a combined experimental and theoretical study on another less known disulfide,  $\text{CF}_3\text{C}(\text{O})\text{OSSOC}(\text{O})\text{CF}_3$ , including theoretical predicted energies and structures of different conformers, vibrational data, and photoelectron spectra. Another aspect of interest in relation to property differences between the neutral molecule and the corresponding cationic-radical form is the geometry of the most stable structure, as well as the rotational barrier of the S–S bond in this molecule.

## Experimental Section

**Sample Preparation.** Bis(trifluoroaceto) disulfide was prepared from sulfur monochloride ( $\text{S}_2\text{Cl}_2$ )<sup>19</sup> and silver trifluoroacetate ( $\text{AgOC}(\text{O})\text{CF}_3$ , Aldrich) according to Wang et al.<sup>20</sup>  $\text{AgOC}(\text{O})\text{CF}_3$  was dried in a vacuum at 50 °C before experiment. Trap-to-trap separation was needed to remove a minor impurity of anhydride. The yield is greater than 90%. The purity was checked by liquid-phase infrared spectroscopy as well as mass spectrometry. The title compound is moisture sensitive and decomposes to give trifluoroacetic anhydride,  $\text{CF}_3\text{C}(\text{O})\text{OC}(\text{O})\text{CF}_3$ , sulfur dioxide, and sulfur.

**Raman Spectroscopy.** The sample in a 4 mm glass capillary was excited with 200 mW of  $\text{Ar}^+$  laser at 488 nm (Spectra-Physics Beam Lock). The Raman was collected and focused into a spectrometer (SpectraPro-500i, Acton) equipped with a liquid nitrogen cooled CCD detection system (SPEC-10-400B/LbN, Roper Scientific).

**Photoelectron Spectroscopy.** The PE spectrum was recorded on a double-chamber UPS-II instrument, which was designed specifically to detect transient species as described elsewhere<sup>21,22</sup> at a resolution of about 30 meV as indicated by the  $\text{Ar}^+(\text{P}_{2/3})$  photoelectron band. Experimental vertical ionization potentials (IP in eV) are calibrated by simultaneous addition of a small amount of argon and methyl iodide to the sample.

**Quantum Chemical Calculations.** The calculations were performed with the Gaussian98 programs<sup>23</sup> applied with the ab initio Hartree–Fock (HF) and the MP2 methods as well as the density function B3LYP approach, in which Becke's three parameter hybrid functional,<sup>24</sup> representing the exchange term, is combined with the correlation functional of Lee, Yang, and Parr.<sup>25</sup> Vibrational-frequency calculations for neutral and cationic-radical states have been carried out to verify stationary points. The vertical ionization energies (eV) for all conformers were calculated at the ab initio level according to Cederbaum's outer valence Green's function (OVGF)<sup>26</sup> method at 6-31G basis set. The adiabatic energy was obtained according to the energy differences between the most stable conformer and the corresponding cationic-radical form. The Mulliken population analysis was applied for assigning charges for both neutral and cationic-radical forms.

## Results and Discussion

**(a) Geometry of  $\text{CF}_3\text{C}(\text{O})\text{OSSOC}(\text{O})\text{CF}_3$ .** The chalcogen–chalcogen bonds in bivalent compounds are known to prefer gauche conformations, with typical dihedral angles of 80–90°, which is usually attributed to lone-pair interactions.<sup>9</sup> Ab initio and experimental studies on  $\text{CH}_3\text{OSSOCH}_3$  indicated that three conformers resulting from the rotation of S–O and S–S bands should be stable.<sup>7–9</sup> Meanwhile, recently reported new compound  $\text{CF}_3\text{C}(\text{O})\text{SOC}(\text{O})\text{CF}_3$  was calculated to possess a skew structure,<sup>27</sup> with C=O bonds of both  $\text{CF}_3\text{C}(\text{O})$  groups anti- or synperiplanar to the S–O bond, and four conformers were predicted to be stable theoretically, with the syn-syn (C=O bonds synperiplanar to S–O bond) conformer being the most

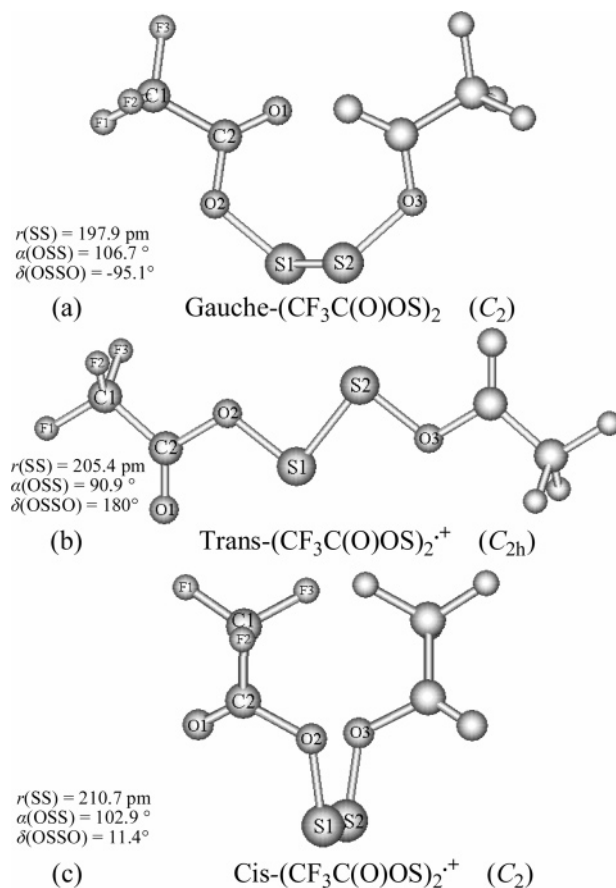


**Figure 1.** Schematic representation of (a) the most stable conformer **1** of *gauche*-( $\text{CF}_3\text{C}(\text{O})\text{OS}$ )<sub>2</sub> ( $C_2$ ), (b) *trans*-( $\text{CF}_3\text{C}(\text{O})\text{OS}$ )<sub>2</sub><sup>+</sup> ( $C_{2h}$ ), and (c) *cis*-( $\text{CF}_3\text{C}(\text{O})\text{OS}$ )<sub>2</sub><sup>+</sup> ( $C_2$ ) at the B3LYP/6-311G\* level of theory.

stable. As for  $\text{CF}_3\text{C}(\text{O})\text{OSSOC}(\text{O})\text{CF}_3$ , the above two aspects should be considered for seeking the most stable conformer on its potential energy surface.

Referring to the most stable conformers of  $\text{CH}_3\text{OSSOCH}_3$  and  $\text{CF}_3\text{C}(\text{O})\text{SOC}(\text{O})\text{CF}_3$ , a conformer with the dihedral angle  $\delta_{\text{OSSO}} = -90^\circ$ , *gauche* symmetry, and both C=O groups *cis* to S–O was assumed; then, it was set as the starting geometry for quantum chemical optimizations with different levels of theory. A stable conformer **1** with  $C_2$  symmetry (Figure 1) was found to be a real minimum, and fully optimized at HF, B3PW91, and B3LYP methods. To determine other possible conformers with different values of  $\delta_{\text{OSSO}}$ , a relax scan of the potential energy surface was performed by rotating the torsional dihedral angle  $\delta_{\text{OSSO}}$  in steps of 10° using HF/6-31G\* and B3LYP/6-31G\* approximation, while keeping the structures of  $\text{CF}_3\text{C}(\text{O})\text{O}$  moieties optimized. The resulting potential curves for dihedral angles from 0° to 360° are shown in Figure 2. The profile displays two minima near  $\delta_{\text{OSSO}} = 90^\circ$  and  $\delta_{\text{OSSO}} = 270^\circ$  (or  $-90^\circ$ ) at both theoretical levels, respectively. Subsequently, the conformer with  $\delta_{\text{OSSO}} = 90^\circ$  was fully optimized using the same methods as conformer **1**, and was confirmed to be another stable conformer **5** of  $\text{CF}_3\text{C}(\text{O})\text{OSSOC}(\text{O})\text{CF}_3$  with the same  $C_2$  symmetry by vibrational analysis.

By changing the relative orientation of C=O and S–O bonds, eight other different conformers were also found. A scheme of all 10 conformers (**1**–**10**) is presented in Figure 3, and the relative energies with different levels of theory are also listed in Table 1. It can be clearly seen that the energy differences are small among conformers, with **1** being the global minimum. Conformer **1** exhibits 0.13 kcal mol<sup>-1</sup> in energy lower than the second stable conformer **9** at the B3LYP/6-311G\* level. As is

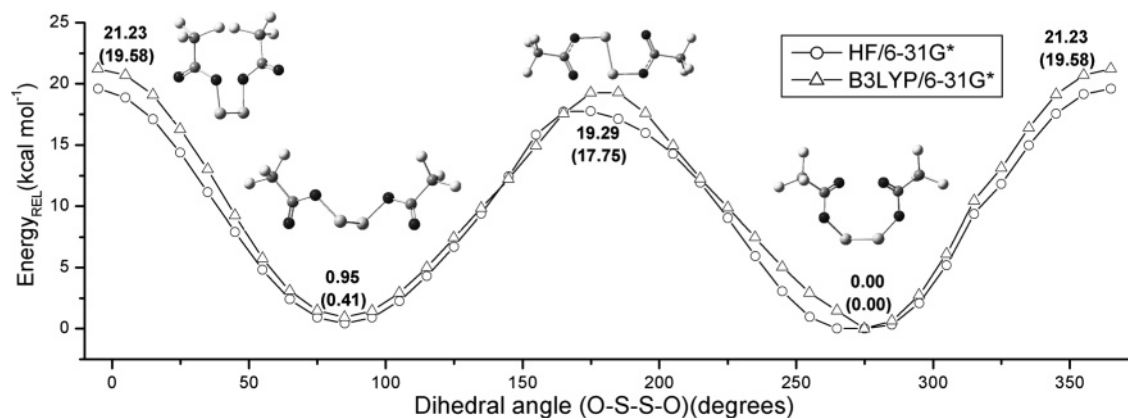


**Figure 2.** Conformational energy profile for bis(trifluoroaceto) disulfide obtained using the relax scan of potential energy surface (rotating the OSSO dihedral in steps of 10°) at the HF/6-31G\* and B3LYP/6-31G\* levels.

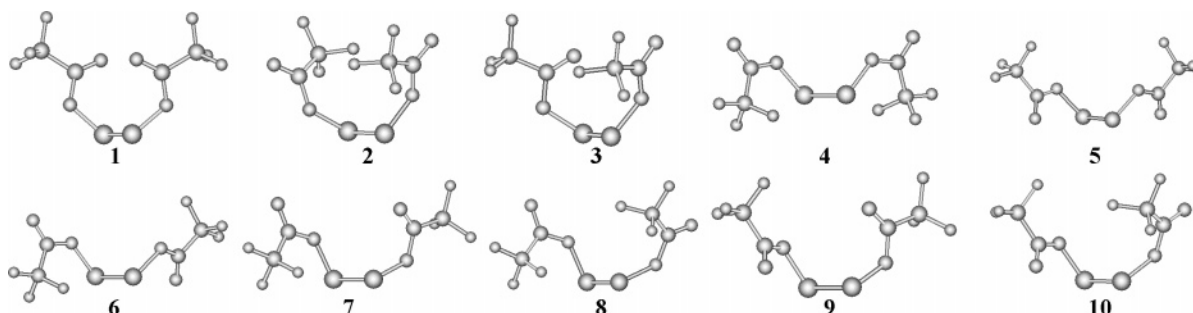


**Figure 3.** Schematic representation of 10 conformers (1–10) of  $\text{CF}_3\text{C}(\text{O})\text{OSSOC}(\text{O})\text{CF}_3$ .

**TABLE 1: Calculated Relative Energies ( $\text{kcal mol}^{-1}$ ) of Different Conformers of  $\text{CF}_3\text{C}(\text{O})\text{OSSOC}(\text{O})\text{CF}_3$**

method	HF 6-31+G*	B3PW91 6-31+G*	MP2 6-31G*	B3LYP 6-31+G*	B3LYP 6-311G*
<b>1</b>	0	0	0	0	0
<b>2</b>	18.45	12.80	13.97	13.18	12.83
<b>3</b>	9.31	7.17	7.46	6.87	6.34
<b>4</b>	19.16	13.69	15.93	13.45	13.30
<b>5</b>	0.70	0.33	1.61	0.53	0.33
<b>6</b>	9.39	7.19	7.51	6.90	6.84
<b>7</b>	9.73	7.28	8.78	7.16	7.05
<b>8</b>	18.74	13.54	15.32	13.31	13.10
<b>9</b>	0.30	0.10	0.78	0.37	0.13
<b>10</b>	9.18	6.85	6.84	6.85	6.28

evident from Figure 2, although the energy differences between conformers of **1** and **5** is less than 1.0  $\text{kcal mol}^{-1}$ , the energy barrier for the S–S rotation is calculated to be much higher as 17.75 (HF/6-31G\*) and 19.29 (B3LYP/6-31G\*)  $\text{kcal mol}^{-1}$ . Recently, it has been reported that the disulfide rotation barrier is doubled by replacing the carbon in CSSC (ca. 7  $\text{kcal mol}^{-1}$ ) with electronegative oxygen to give the dialkoxy disulfide moiety OSSO ( $\Delta G_{\text{rot}}^\ddagger = 18\text{--}19 \text{ kcal mol}^{-1}$ ).<sup>28</sup> Restricted rotation about a single bond is not usually influenced solely through stereoelectronic interactions. For instance, well-documented high torsional barriers in amides,<sup>29</sup> thioamides,<sup>30</sup> sulfenamides,<sup>31</sup> acrylonitriles (DMAAN),<sup>32</sup> and carbamates<sup>33</sup> are due to in part the resonance-induced double bond character in these systems.<sup>34</sup> The extremely high rotation barrier in  $\text{CF}_3\text{C}(\text{O})\text{OSSOC}(\text{O})\text{CF}_3$  arises partially from the contracted S–S bond, which is calculated to be 1.979 Å at the B3LYP/6-311G\* level, in comparison to 2.031(3) Å (GED) for  $\text{CH}_3\text{SSCH}_3$ ,<sup>35</sup> 2.027(4) Å (GED) for  $\text{FC}(\text{O})\text{SSCF}_3$ ,<sup>36</sup> and 2.023(3) Å (GED) for  $\text{FC}(\text{O})\text{SSC}(\text{O})\text{CF}_3$ .<sup>37</sup> To our knowledge, the S–S lone pair repulsion and steric interactions between two  $\text{CF}_3\text{C}(\text{O})$  moieties should be taken into account as well. The least stable conformer **4** adopts a structure of both C=O groups trans to the S–O bonds

and lies 13.30  $\text{kcal mol}^{-1}$  (B3LYP/6-311G\*) above conformer **1** in energy; similarly the least stable conformer was also found for  $\text{CF}_3\text{C}(\text{O})\text{SOC}(\text{O})\text{CF}_3$  with anti orientation of C=O to the S–O bond.

The calculated O–S bond length in  $\text{CF}_3\text{C}(\text{O})\text{OSSOC}(\text{O})\text{CF}_3$  is 1.755 Å (B3LYP/6-311G\*), which is longer than other O–S bonds of  $\text{CH}_3\text{OSOCH}_3$  1.625(2) Å,  $\text{CH}_3\text{OSSOCH}_3$  1.650(3) Å,  $\text{CF}_3\text{SOC}(\text{O})\text{CF}_3$  1.663(5) Å, and  $\text{CF}_3\text{SOCF}_3$  1.677 Å.<sup>38,39</sup> An argument for the different lengths of S–O has been postulated by Oberhammer et al.<sup>39</sup> as follows: if the electronegativity of the substituent R at the sulfur atom increases, the polarity of the bond in  $\text{RSOR}'$  is increased and the bond shortens; while, if the electronegativity of the substituent R' at the oxygen increases, the polarity of the bond is decreased and the bond lengthens. The  $\text{CF}_3\text{C}(\text{O})$  substituent on the oxygen and the S atom substituent on the sulfur will lengthen the S–O bond in  $\text{CF}_3\text{C}(\text{O})\text{OSSOC}(\text{O})\text{CF}_3$ .

The optimized geometric parameters for the most stable conformer **1** were given in Table 2. Besides the S–S bond length, another important structural parameter for disulfides is the torsional dihedral  $\delta_{\text{XSSX}}$ , which greatly influenced the whole structure of the molecules investigated. Gas-phase structures of noncyclic disulfides XSSX are characterized by dihedral angles  $\delta_{\text{XSSX}}$  close to 90°: for example,  $\text{H}_2\text{S}_2$  90.6(6)°,  $\text{S}_2\text{F}_2$  87.7(4)°,  $\text{CH}_3\text{SSCH}_3$  85.1(4)°, and  $\text{CH}_3\text{OSSOCH}_3$  91.0(4)°.<sup>9,37</sup> Earlier, Erben et al. reported the smallest dihedral angle  $\delta_{\text{CSSC}} = 77.7\text{--}(21)^\circ$  measured (GED) for noncyclic disulfides in the gas phase of  $\text{FC}(\text{O})\text{SSC}(\text{O})\text{CF}_3$ .<sup>37</sup> The  $\delta_{\text{OSSO}}$  value in  $\text{CF}_3\text{C}(\text{O})\text{OSSOC}(\text{O})\text{CF}_3$  is calculated to be ca.  $-95.1^\circ$ . The interpretation of the population analysis is consistent with two qualitative arguments about the approximate perpendicular orientation of the XSSX dihedral angle. A plausible explanation is related to the resulting barrier formed by the repulsion of the  $3p\pi$  AO lone pairs. The repulsion is minimized if these AOs are oriented orthogonal to each other. Another argument is based on a hyperconjugative



**TABLE 2: Optimized Geometrical Parameters for the Gauche Conformer 1 of CF<sub>3</sub>C(O)OSSOC(O)CF<sub>3</sub> and for the Trans-Planar Cationic-Radical Form of CF<sub>3</sub>C(O)OSSOC(O)CF<sub>3</sub><sup>•+</sup> <sup>a</sup>**

	CF <sub>3</sub> C(O)OSSOC(O)CF <sub>3</sub>				CF <sub>3</sub> C(O)OSSOC(O)CF <sub>3</sub> <sup>•+</sup>	
	HF <sup>b</sup>	B3PW91 <sup>b</sup>	B3LYP <sup>b</sup>	B3LYP <sup>c</sup>	UB3PW91 <sup>b</sup>	UB3LYP <sup>c</sup>
<i>r</i> <sub>CF1F</sub> <sup>d</sup>	1.313	1.338	1.343	1.338	1.328	1.327
<i>r</i> <sub>C1C2</sub>	1.538	1.553	1.556	1.552	1.555	1.557
<i>r</i> <sub>C2O1</sub>	1.173	1.196	1.198	1.189	1.189	1.180
<i>r</i> <sub>C2O2</sub>	1.331	1.349	1.354	1.353	1.394	1.405
<i>r</i> <sub>O2S1</sub>	1.680	1.744	1.757	1.755	1.676	1.684
<i>r</i> <sub>S1S2</sub>	1.985	1.959	1.975	1.979	2.036	2.054
<i>α</i> <sub>FC1F</sub> <sup>d</sup>	108.8	108.7	108.6	108.7	110.1	110.1
<i>α</i> <sub>FC1C2</sub> <sup>d</sup>	110.2	110.2	110.3	110.2	108.8	108.8
<i>α</i> <sub>C1C2O1</sub>	123.6	123.7	123.7	124.0	128.6	129.0
<i>α</i> <sub>C1C2O2</sub>	109.3	108.6	108.6	108.3	109.7	109.0
<i>α</i> <sub>C2O2S1</sub>	119.8	116.8	117.2	117.6	110.2	112.3
<i>α</i> <sub>O2S1S2</sub>	104.6	106.9	106.8	106.7	90.8	90.9
<i>δ</i> <sub>F1C1C2O1</sub>	-3.5	-7.1	-6.4	-4.9	0	0
<i>δ</i> <sub>F2C1C2O1</sub>	116.2	112.4	113.2	114.6	120.3	120.3
<i>δ</i> <sub>F3C1C2O1</sub>	-124.2	-127.8	-127.0	-125.4	-120.3	-120.3
<i>δ</i> <sub>C1C2O2S1</sub>	174.6	174.5	174.8	174.9	180.0	180.0
<i>δ</i> <sub>O1C2O2S1</sub>	-4.7	-4.7	-4.5	-4.6	0	0
<i>δ</i> <sub>C2O2S1S2</sub>	94.4	93.9	93.0	91.8	180.0	180.0
<i>δ</i> <sub>O2S1S2O3</sub>	-92.4	-95.4	-95.1	-95.1	180.0	180.0

<sup>a</sup> Distances in angstroms, angles in degrees. For atom numbering, see Figure 1. <sup>b</sup> At the 6-31+G\* level. <sup>c</sup> At the 6-311G\* level. <sup>d</sup> Average.

**TABLE 3: Atomic Charge for the Neutral and Cationic-Radical (Trans) Form of CF<sub>3</sub>C(O)OSSOC(O)CF<sub>3</sub> as Obtained by the UB3LYP/6-311G\* Approximation**

	atoms <sup>a</sup>								
	F1	F2	F3	C1	C2	O1	O2	S1	TAC <sup>b</sup>
CF <sub>3</sub> C(O)OSSOC(O)CF <sub>3</sub>	-0.18	-0.20	-0.19	0.66	0.30	-0.27	-0.43	0.30	0
CF <sub>3</sub> C(O)OSSOC(O)CF <sub>3</sub> <sup>•+</sup>	-0.14	-0.16	-0.16	0.70	0.29	-0.20	-0.43	0.60	+0.5
<i>Δq</i> <sup>c</sup>	0.04	0.04	0.03	0.03	-0.01	0.07	0.00	0.30	+0.5

<sup>a</sup> For atom numbering, see Figure 1. <sup>b</sup> Total atomic charge. <sup>c</sup>  $\Delta q = q(\text{CF}_3\text{C(O)OSSOC(O)CF}_3^{\bullet+})/2 - q(\text{CF}_3\text{C(O)OSSOC(O)CF}_3)/2$ .

mechanism, where the  $\pi$ -character of the S–S bond is enhanced, when S–X bonds (S–O in CF<sub>3</sub>C(O)OSSOC(O)CF<sub>3</sub>) are aligned for maximum transfer of electron density through the 3p $\pi$  AOs to the X atom. This feature is consistent with the anomeric effects, that is, the electron donation from the sulfur lone pair into the empty  $\sigma^*$  orbitals of the opposite S–X bonds. However, in the case of peroxides, the values for  $\delta_{\text{XOOX}}$  show larger variation. In the parent compound, H<sub>2</sub>O<sub>2</sub>, the value amounts to 119.8° (MW)<sup>40</sup> (the more recent reported  $\delta_{\text{HOOH}}$  is 112°<sup>41</sup>), but surprisingly small torsional angles are possessed by the peroxides F<sub>2</sub>O<sub>2</sub> 88.1(4)°,<sup>42</sup> Cl<sub>2</sub>O<sub>2</sub> 81.0(1)°,<sup>43</sup> as well as two sp<sup>2</sup>-hybridized substituents, that is, FC(O)OOC(O)F 83.5(14)°<sup>44</sup> and CF<sub>3</sub>C(O)OOC(O)CF<sub>3</sub> 86.5(32)°.<sup>45</sup>

Meanwhile, the  $\delta_{\text{O1C2O2S1}}$  (Figure 1) in CF<sub>3</sub>C(O)OSSOC(O)CF<sub>3</sub> is calculated to be -4.6°, which corresponds to -3.6° (B3LYP/6-31G\*) for the  $\delta_{\text{OCOS}}$  of CF<sub>3</sub>C(O)SOC(O)CF<sub>3</sub>.<sup>27</sup> The  $\delta_{\text{C2O2S1S2}}$  is 91.8°, close to those of the most recently reported  $\delta_{\text{COSC}}$  in CF<sub>3</sub>SOC(O)CH<sub>3</sub> 100.3(40)° and CF<sub>3</sub>SOC(O)CF<sub>3</sub> 101.1(27)°, respectively.<sup>39</sup>

**(b) Geometry of CF<sub>3</sub>C(O)OSSOC(O)CF<sub>3</sub><sup>•+</sup>.** Upon ionization, the CSSC dihedral angle in CH<sub>3</sub>SSCH<sub>3</sub> (85.1(4)°) is expected to change to 180° in CH<sub>3</sub>SSCH<sub>3</sub><sup>•+</sup> in the ground state, and this most stable conformer exhibits C<sub>2h</sub> trans symmetry. Interestingly, a stable structure with a C<sub>2v</sub> symmetry (*cis*-CH<sub>3</sub>-SSCH<sub>3</sub><sup>•+</sup>, CSSC dihedral angle = 0°) is also found, and it lies only 0.17 eV above the ground C<sub>2h</sub> structure.<sup>15</sup> Recently, the structures of ground-state FC(O)SSMe<sup>•+</sup> have been studied by Erben et al.<sup>18</sup> It was concluded that, after ionization, the  $\delta_{\text{SSCO}}$  dihedral is retained, but the  $\delta_{\text{CSSC}}$  adopts a value of 180°. Enlightened by both studies, we located two stable conformers of the ground cationic-radical form CF<sub>3</sub>C(O)OSSOC(O)CF<sub>3</sub><sup>•+</sup> (Figure 1) at the UB3PW91/6-31+G\* and UB3LYP/6-311G\* levels of theory. The trans conformer with respect to the

$\delta_{\text{O2S1S2O3}}$  dihedral angle has a planar main-atom structure (180°) with C<sub>2h</sub> symmetry, whereas the *cis* conformer possesses C<sub>2</sub> symmetry, and the  $\delta_{\text{O2S1S2O3}}$  is 11.4°, a little deviated from planar; the deviation arises from the stereo repulsion forces of the CF<sub>3</sub> moieties on the two halves of the molecule. The planar C<sub>2h</sub> conformer is only 0.02 kcal mol<sup>-1</sup> lower in energy than the latter C<sub>2</sub> conformer at the UB3LYP/6-311G\* level (including ZPE corrections).

The calculated geometric parameters (UB3PW91/6-31+G\* and UB3LYP/6-311G\*) for the planar C<sub>2h</sub> conformer of ground cationic-radical form CF<sub>3</sub>C(O)OSSOC(O)CF<sub>3</sub><sup>•+</sup> are given in Table 2 for comparison with those of the corresponding neutral molecule. Obvious changes can be seen in bond lengths with respect to the *r*<sub>O2S1</sub> and *r*<sub>S1S2</sub>: the former bond shortens 0.07 Å while the latter elongates 0.08 Å to exceed 2.0 Å after ionization. The Mulliken population analysis of the charges for both neutral and cationic-radical forms is shown in Table 3. The results demonstrate that the atomic charges are delocalized all over the molecule, with an appreciable fraction localized on the sulfur atom. It can be deduced that the first ionization happens primarily on the electrons of the sulfur atoms, that is, the sulfur 3p lone pair electrons. This ionization process will reasonably elongate the contracted pseudo-double bond of S–S in the neutral molecule. The shortening of the S–O bond is explained by a bond reinforcement when the sulfur exhibits more positive charge in comparison to that of the neutral molecule, while the charges on the neighboring oxygen atom remain unchanged (Table 3). Similar to CH<sub>3</sub>SSCH<sub>3</sub><sup>•+</sup> and FC(O)SSCH<sub>3</sub><sup>•+</sup>,<sup>15,18</sup> the decrease of the sulfur–sulfur lone repulsion after ionization also makes a stable planar structure ( $\delta_{\text{O2S1S2O3}} = 180^\circ$ ) possible for CF<sub>3</sub>C(O)OSSOC(O)CF<sub>3</sub><sup>•+</sup>.

**(c) Vibration Spectroscopy.** The infrared spectrum of CF<sub>3</sub>C(O)OSSOC(O)CF<sub>3</sub> was reported by Wang et al.<sup>20</sup> However, no

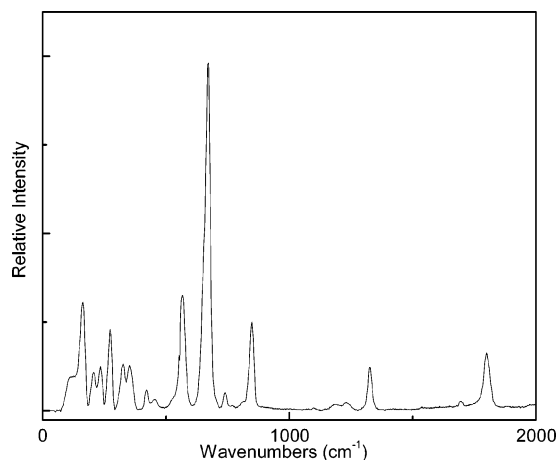


**Figure 4.** Raman spectrum of liquid  $\text{CF}_3\text{C}(\text{O})\text{OSSOC}(\text{O})\text{CF}_3$  at room temperature.

**TABLE 4: Experimental and Calculated Vibrational Wavenumbers ( $\text{cm}^{-1}$ ) of  $\text{CF}_3\text{C}(\text{O})\text{OSSOC}(\text{O})\text{CF}_3$**

mode	assignments	IR		Raman	
		exptl <sup>a,b</sup>	calcd <sup>c</sup>	exptl <sup>a,b</sup>	int <sup>d</sup>
$\nu_1$	$\nu(\text{C}=\text{O})$	1812 m	1877 (287.5)	1799 m	3.6
$\nu_2$	$\nu(\text{C}=\text{O})$		1860 (159.6)		10.9
$\nu_3$	$\nu(\text{C}-\text{C})/\nu_s(\text{CF}_3)$	1326 m	1302 (3.5)	1326 m	16.8
$\nu_4$	$\nu(\text{C}-\text{C})/\nu_s(\text{CF}_3)$		1297 (109.1)		17.8
$\nu_5$	$\nu_{\text{as}}(\text{CF}_3)$	1238 s	1230 (383.3)	1230 w	6.8
$\nu_6$	$\nu_{\text{as}}(\text{CF}_3)$		1227 (252.9)		3.8
$\nu_7$	$\nu_{\text{as}}(\text{CF}_3)$	1196 s	1179 (467.7)	1185 w	2.6
$\nu_8$	$\nu(\text{C}-\text{O})/\nu_s(\text{CF}_3)$	1117 w	1100 (588.2)		<1
$\nu_9$	$\nu(\text{C}-\text{O})/\nu_s(\text{CF}_3)$	1049 s	1068 (477.3)	1096 vw	2.7
$\nu_{10}$	$\delta_s(\text{C}(\text{O})\text{O})/\nu_s(\text{CF}_3)$	998 w	858 (3.1)	848 m	8.6
$\nu_{11}$	$\delta_s(\text{C}(\text{O})\text{O})/\nu_s(\text{CF}_3)$	865 w	845 (17.8)	806 sh	<1
$\nu_{12}$	oop(CC(O)O)	731 m	777 (2.3)	739 w	<1
$\nu_{13}$	oop(CC(O)O)		773 (30.8)		<1
$\nu_{14}$	$\delta_s(\text{C}(\text{O})\text{O})/\nu_s(\text{CF}_3)$		740 (32.3)		1.0
$\nu_{15}$	$\delta_s(\text{C}(\text{O})\text{O})/\nu_s(\text{CF}_3)$		733 (89.6)		<1
$\nu_{16}$	$\nu(\text{S}-\text{O})$	622 m	647 (22.9)	671 vs	47.7
$\nu_{17}$	$\nu(\text{S}-\text{O})/\delta_s(\text{CF}_3)$		629 (80.9)		18.8
$\nu_{18}$	$\delta_{\text{as}}(\text{CF}_3)/\nu(\text{S}-\text{O})$		557 (<1)		7.0
$\nu_{19}$	$\delta_{\text{as}}(\text{CF}_3)/\nu(\text{S}-\text{O})$		550 (25.2)		3.7
$\nu_{20}$	$\delta_{\text{as}}(\text{CF}_3)$		521 (1.6)		<1
$\nu_{21}$	$\nu_s(\text{S}-\text{S})$		519 (13.1)	568 s	14.0
$\nu_{22}$	$\nu_s(\text{S}-\text{S})$		508 (27.6)	524 sh	6.5
$\nu_{23}$	$\delta(\text{CF}_3\text{C}(\text{O}))/\delta_{\text{as}}(\text{CF}_3)$		413 (2.0)	453 w	1.8
$\nu_{24}$	$\delta_{\text{as}}(\text{CF}_3)/\delta(\text{CF}_3\text{C}(\text{O}))$		411 (<1)		<1
$\nu_{25}$	$\delta(\text{COS})/\rho_s(\text{CF}_3)$		356 (6.4)	422 w	1.8
$\nu_{26}$	$\delta(\text{CF}_3\text{C}(\text{O}))/\delta_{\text{as}}(\text{CF}_3)$		347 (3.2)	419 w	2.5
$\nu_{27}$	$\rho_s(\text{CF}_3)/\delta(\text{COS})$		323 (4.0)	352 m	3.7
$\nu_{28}$	$\rho_s(\text{CF}_3)/\delta(\text{COS})$		300 (7.9)	326 m	1.3
$\nu_{29}$	$\delta(\text{OSS})/\rho(\text{CF}_3\text{C}(\text{O}))$		266 (13.5)	274 s	8.8
$\nu_{30}$	$\delta(\text{OSS})/\rho_s(\text{CF}_3)$		262 (15.9)		<1
$\nu_{31}$	$\delta(\text{OSS})/\rho_{\text{as}}(\text{CF}_3)$		225 (<1)	234 m	4.2
$\nu_{32}$	$\delta(\text{OSS})/\rho(\text{CF}_3\text{C}(\text{O}))$		195 (5.1)	205 m	2.8
$\nu_{33}$	$\tau(\text{C}-\text{O})$		148 (<1)	163 s	<1
$\nu_{34}$	$\tau(\text{S}-\text{O})$		145 (<1)	121 sh	<1

<sup>a</sup> Values are taken from ref 20. <sup>b</sup> Key: vs, very strong; s, strong; m, medium; w, weak; vw, very weak; sh, shoulder. <sup>c</sup> Calculated infrared intensities in  $\text{km mol}^{-1}$  at the B3LYP/6-311G\* level based on the gauche conformer **1** of  $\text{CF}_3\text{C}(\text{O})\text{OSSOC}(\text{O})\text{CF}_3$ . <sup>d</sup> Calculated Raman intensities in  $\text{\AA}^4 \text{u}^{-1}$ .

detailed assignments, Raman spectrum, and theoretical calculations have been reported for this molecule. Figure 4 presents the liquid-phase Raman spectrum of  $\text{CF}_3\text{C}(\text{O})\text{OSSOC}(\text{O})\text{CF}_3$ . In Table 4, all vibrational data observed are collected together with the theoretically predicted wavenumbers (B3LYP/6-311G\*) for the most stable conformer **1** and the corresponding assignments. The vibrational modes were assigned in comparison with

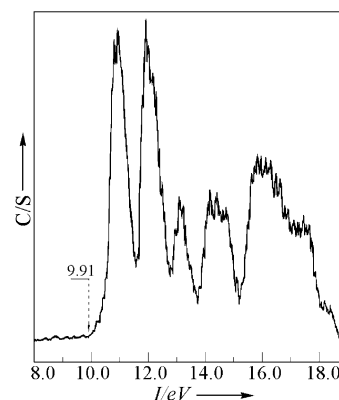


**Figure 5.** HeI photoelectron spectrum (PES) of  $\text{CF}_3\text{C}(\text{O})\text{OSSOC}(\text{O})\text{CF}_3$ .

**TABLE 5: Calculated Ionization Energies (eV) for Different Conformers of  $\text{CF}_3\text{C}(\text{O})\text{OSSOC}(\text{O})\text{CF}_3$**

isomer	ROVGF/6-31G								
<b>1</b>	10.99	11.27	12.20	12.34	12.29	13.22	14.17	14.59	14.94
<b>2</b>	10.84	10.96	11.82	12.11	12.57	13.11	13.75	14.89	16.25
<b>3</b>	11.20	11.43	12.78	13.34	13.54	14.52	14.85	15.25	15.56
<b>4</b>	10.90	10.91	11.86	12.14	12.53	13.19	14.03	14.68	14.82
<b>5</b>	11.06	11.18	12.12	12.34	12.48	13.47	14.54	14.55	14.75
<b>6</b>	11.23	11.44	12.72	13.36	13.50	14.52	15.07	15.31	15.35
<b>7</b>	11.18	11.45	12.72	13.32	13.50	14.54	15.01	15.08	15.42
<b>8</b>	11.17	11.40	12.64	13.40	13.42	14.44	15.00	15.07	15.53
<b>9</b>	11.23	11.46	12.81	13.43	13.52	14.69	15.10	15.11	15.43
<b>10</b>	11.22	11.44	12.71	13.38	13.51	14.53	15.13	15.15	15.54

the theoretical wavenumbers and intensities as well as relevant reported data.

The vibrational spectra show characteristic bands corresponding to the  $\text{C}=\text{O}$  stretching vibration at 1812 (IR) and 1799 (Raman)  $\text{cm}^{-1}$ ; to the  $\text{C}-\text{F}$  vibrations at 1238 (IR) and 1230 (Raman)  $\text{cm}^{-1}$ ; to the  $\text{C}-\text{O}$  bonds at 1049 (IR) and 1096 (Raman)  $\text{cm}^{-1}$ ; to the  $\text{S}-\text{O}$  stretching vibration at 622 (IR) and 671 (Raman)  $\text{cm}^{-1}$ ; and to the  $\text{S}-\text{S}$  stretching vibrations at 568 and 524  $\text{cm}^{-1}$  (Raman). Because the stretching modes of the COSSOC chain and bending modes of the COSSOC skeleton have been discussed detailed in analyzing the vibrational spectra of  $\text{CH}_3\text{OSSOCH}_3$ ,<sup>9</sup> other assignments of vibrational modes were accomplished by referring to it as well as features reported for  $\text{CF}_3\text{C}(\text{O})\text{SOC}(\text{O})\text{CF}_3$ ,<sup>27</sup>  $\text{FC}(\text{O})\text{SSC}(\text{O})\text{CF}_3$ ,<sup>37</sup> and  $\text{CF}_3\text{SOC}(\text{O})\text{CF}_3$ .<sup>39</sup>

**(d) Photoelectron Spectroscopy.** The HeI photoelectron spectrum of  $\text{CF}_3\text{C}(\text{O})\text{OSSOC}(\text{O})\text{CF}_3$  is shown in Figure 5. Before assigning the spectrum, ROVGF calculations were carried out to obtain the ionization energies for the 10 theoretically stable conformers (**1**–**10**). The results are listed in Table 5. Since the 10 conformers with comparable energies are possible in some cases, first we should investigate whether the spectrum can originate from a mixture of all the conformers or some of them dominate. However, in comparison to the calculated orbital energies, we reduced our discussions to the analysis of the global minimum  $C_2$  conformer **1**. The experimental vertical ionization potentials (IP in eV), theoretical vertical ionization energies ( $E_v$  in eV), molecular orbitals, and corresponding characters of outer valence shells for the most stable conformer **1** with OVG methods are listed in Table 6.

As pointed out by Baker et al.,<sup>46</sup> for disulfides, peroxides, and diselenides, the first two bands in the photoelectron spectra correspond to the symmetric and antisymmetric linear combinations of the outermost p-atomic orbitals, producing orbitals  $p\pi$  and  $p\pi^*$ , respectively. The first broad band (Figure 5) with high

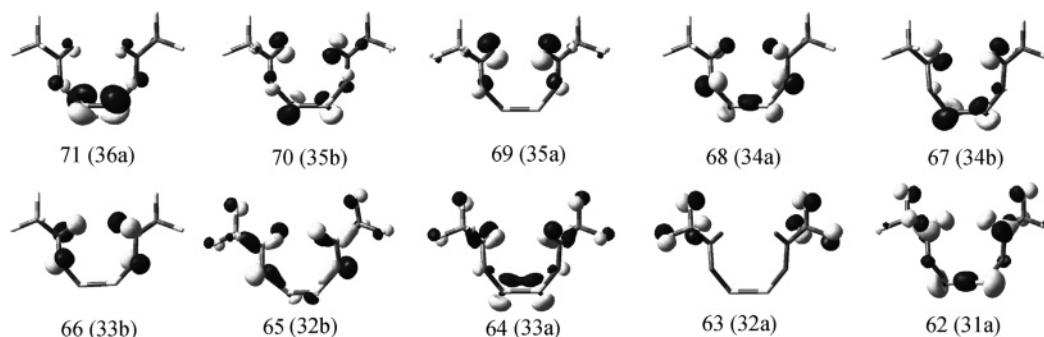


**Figure 6.** Drawings of the first ten HOMOs for the gauche conformer **1** of  $\text{CF}_3\text{C}(\text{O})\text{OSSOC}(\text{O})\text{CF}_3$ .

**TABLE 6: PES Vertical Ionization Energies (IP in eV), Computed Vertical Ionization Energies ( $E_v$  in eV) by ROVGF/6-31G Calculations, and Molecular Orbital Character for the Gauche Conformer **1** of  $\text{CF}_3\text{C}(\text{O})\text{OSSOC}(\text{O})\text{CF}_3$**

exptl IP	calcd $E_v^a$	MO	character
10.81	10.99 (0.92)	36a	$n^{\text{A}}_{\text{S}}$
10.97	11.27 (0.92)	35b	$n^{\text{B}}_{\text{S}}, n^{\text{B}}_{\text{O}(\text{C}=\text{O})}$
11.95	12.20 (0.91)	35a	$n^{\text{A}}_{\text{O}(\text{C}=\text{O})}, n^{\text{A}}_{\text{O}(\text{COS})}$
12.16	12.29 (0.90)	34a	$n^{\text{A}}_{\text{O}(\text{COS})}, \sigma^{\text{A}}_{(\text{S}-\text{S})}$
12.38	12.34 (0.90)	34b	$n^{\text{B}}_{\text{S}}, n^{\text{B}}_{\text{O}(\text{C}=\text{O})}$
13.10	13.22 (0.89)	33b	$n^{\text{B}}_{\text{O}(\text{C}=\text{O})}, n^{\text{B}}_{\text{O}(\text{COS})}$
14.15	14.17 (0.90)	32b	$n^{\text{B}}_{\text{O}(\text{COS})}, \sigma^{\text{B}}_{(\text{C}=\text{O})}$
14.42	14.59 (0.89)	33a	$n^{\text{B}}_{\text{S}}, \pi^{\text{B}}_{(\text{C}=\text{O})}$
14.69	14.94 (0.90)	32a	$n^{\text{A}}_{\text{F}}$
15.90	15.95 (0.92)	31a	$\sigma^{\text{A}}_{(\text{S}-\text{S})}, n^{\text{A}}_{\text{F}}$
	15.99 (0.91)	31b	$n^{\text{B}}_{\text{F}}$
	16.05 (0.90)	30b	$n^{\text{B}}_{\text{F}}$
16.42	16.34 (0.92)	30a	$n^{\text{A}}_{\text{F}}$

<sup>a</sup> Pole strength in parentheses.

intensity can overlap two peaks at 10.81 and 10.97 eV. The population analysis (Figure 6) shows that the main characters for the first two outermost orbitals are  $\{36a (n^{\text{A}}_{\text{S}})\}^{-1}$  and  $\{35b (n^{\text{B}}_{\text{S}}, n^{\text{B}}_{\text{O}(\text{C}=\text{O})})\}^{-1}$ , and the theoretically predicted first two vertical ionization energies are 10.99 and 11.19 eV, respectively, in good agreement with the experimental observed values. Apparently, the latter antisymmetric combination of the sulfur 3p lone pair orbitals was influenced by the participation of the carbonyl oxygen lone pair as depicted in Figure 6. The energy separation  $\Delta E$  between the  $p\pi$  and the  $p\pi^*$  orbitals in this molecule is 0.16 eV ( $\delta_{\text{OSSO}} = -95.1^\circ$ ), which is smaller than those of  $\text{CH}_3\text{SSCH}_3$  ( $\Delta E = 0.30$  eV,  $\delta_{\text{CSSC}} = 85.1(4)^\circ$ ) and  $t\text{-Bu}_2\text{S}_2$  ( $\Delta E = 0.65$  eV,  $\delta_{\text{CSSC}} = 84.5(5)^\circ$ ).<sup>16</sup> In general, it is to be expected that as the dihedral angle  $\delta$  deviates from  $90^\circ$ , the energy separation  $\Delta E$  between the  $p\pi$  and the  $p\pi^*$  orbitals will increase, i.e., the 3p orbitals in parallel configuration ( $\delta = 0^\circ, 180^\circ$ ) interact more strongly than in an orthogonal configuration ( $\delta = 90^\circ$ ).<sup>47</sup> It is interesting to note that the first two highest occupied molecular orbitals (HOMOs) of conformers **1**, **4**, and **10** are different as outlined in Figure 7. In the  $C_2$  conformer **4**, the first HOMO is more likely the antibonding linear combination of the  $3p\pi$ -MOs, but the second is the bonding linear combination of the  $3p\pi$ -MOs; both orbitals show an inversion compared to those of the  $C_2$  conformer **1**. As for the  $C_1$  conformer **10**, the 3p lone pair electrons of the two sulfur atoms are separated into two HOMOs, with a calculated difference of 0.22 eV (Table 5). It should be attributed to the influence of the conformation as well as the breakdown of the molecular symmetry.

According to the Franck–Condon principle, the change of the conformation after ionization makes the adiabatic ionization energy not identical to the corresponding vertical ionization

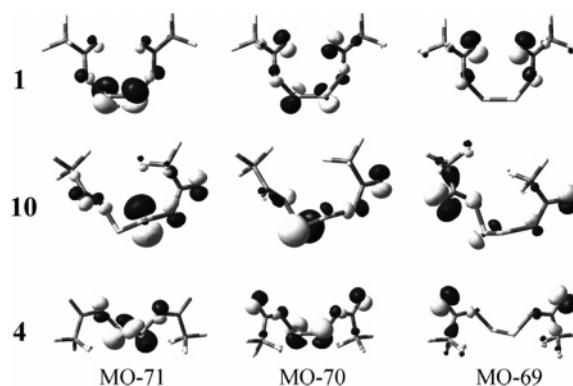


**Figure 7.** Drawings of the first three HOMOs of three isomers of  $\text{CF}_3\text{C}(\text{O})\text{OSSOC}(\text{O})\text{CF}_3$ : **1**, **10**, and **4** respectively.

energy.<sup>17</sup> Although very poor Franck–Condon factors for the ionization transition near the threshold are displayed by several sulfur-containing compounds,<sup>7,17</sup> an adiabatic ionization energy of 9.91 eV still can be obtained from the PE spectrum of  $\text{CF}_3\text{C}(\text{O})\text{OSSOC}(\text{O})\text{CF}_3$  as is shown in Figure 5. This value is in good agreement with the value 9.90 eV calculated from the difference between the energies of the neutral conformer **1** and the ground cationic-radical  $\text{trans}-(\text{CF}_3\text{C}(\text{O})\text{OS})_2^{\bullet+}$  (Figure 1) at the B3LYP/6-311G\* level of theory.

The second band with high intensity is also the result of several overlapping ionization processes. With the aid of ROVGF calculations (Table 6) and population analysis (Figure 6), three ionization processes are included in this ionization region:  $\{35a (n^{\text{A}}_{\text{O}(\text{C}=\text{O})}, n^{\text{A}}_{\text{O}(\text{COS})})\}^{-1}$ ,  $\{34a (n^{\text{A}}_{\text{O}(\text{COS})}, \sigma^{\text{A}}_{(\text{S}-\text{S})})\}^{-1}$ , and  $\{34b (n^{\text{B}}_{\text{S}}, n^{\text{B}}_{\text{O}(\text{C}=\text{O})})\}^{-1}$ , at 11.95, 12.16, and 12.38 eV, respectively. The same component in these orbitals is the oxygen lone pair electrons; similar ionizations also happen in other carbonyl compounds and formates<sup>48</sup> in this energy region. The third band centered at 13.10 eV also comes from the oxygen lone-pair ionizations and corresponds to the ionization energy of 12.92 eV for  $\text{CF}_3\text{C}(\text{O})\text{OH}$ .<sup>48</sup> The bands at higher energies between 14.5 and 18.0 eV show broad signals; they are characteristic of ionizing the fluorine lone pair electrons  $n_{\text{F}}$  of the  $\text{CF}_3$  groups. These unresolved signals make a further assignment difficult. The main characters of these orbitals are depicted in Figure 6.

## Conclusion

Bis(trifluoroaceto) disulfide  $\text{CF}_3\text{C}(\text{O})\text{OSSOC}(\text{O})\text{CF}_3$  was prepared and characterized by Raman, photoelectron spectroscopy (PES), and quantum chemical calculations. This molecule exhibits the same general trend observed in previous conformational studies of esters ( $-\text{C}(\text{O})\text{O}-$ ) and disulfides ( $-\text{SS}-$ ). The gauche conformer **1** with both  $\text{C}=\text{O}$  bonds cis to the  $\text{S}-\text{S}$  bonds is energetically preferred over the other conformers.



Moreover, the structure of the OSSO moiety is characterized by a gauche dihedral angle  $\delta_{O_2S_1S_2O_3} = -95.1^\circ$  due to the sulfur–sulfur lone pair interactions. The contracted S–S bond (1.979 Å) and relatively high rotational barrier of the  $\delta_{OSSO}$  (ca. 19.29 kcal mol<sup>-1</sup> at B3LYP/6-31G\* level) indicates the partial resonance-induced double bond character in this molecule.

After ionization, the cationic-radical form CF<sub>3</sub>C(O)OSSOC(O)CF<sub>3</sub><sup>•+</sup> adopts a trans planar main-atom structure ( $\delta_{O_2S_1S_2O_3} = 180^\circ$  and  $\delta_{O_1C_2O_2S_1} = 0^\circ$ ) with C<sub>2h</sub> symmetry. The S–S bond elongates to 2.054 Å, while the S–O bond shortens from 1.755 Å in its neutral form to 1.684 Å in the cationic-radical form. This ionization corresponds to the leaving electrons mainly localized on the sulfur 3p lone pair orbitals:  $3p\pi \{36a (n^A_S)\}^{-1}$  and  $3p\pi^* \{35b (n^B_S, n^B_{O(C=O)})\}^{-1}$ , with an energy separation of 0.16 eV. The first vertical ionization energy is 10.81 eV, which is not identical with the first adiabatic ionization energy 9.91 eV, due to the geometric change after ionization. Meanwhile, another less stable *cis*-CF<sub>3</sub>C(O)OSSOC(O)CF<sub>3</sub><sup>•+</sup> with C<sub>2</sub> symmetry is also obtained theoretically.

**Acknowledgment.** This project was supported by the Chinese Academy of Sciences (Contract No: KJXC2-SW-H8 and Hundred talents fund) and the National Natural Science Foundation of China (Contracts 20477047, 20473094, 50372071, 20577052). X.Z. thanks the Chinese Academy of Sciences for a scholarship during the period of this work. The authors also thank Qing Liao for Raman measurement.

**Supporting Information Available:** Optimized structures and parameters for *cis*- and *trans*-CF<sub>3</sub>C(O)OSSOC(O)CF<sub>3</sub><sup>•+</sup>. This material is available free of charge via the Internet at <http://pubs.acs.org>.

## References and Notes

- (1) Lengfeld, F. *Chem. Ber.* **1895**, 28, 449
- (2) Borghi, R.; Lunazzi, L.; Placucci, G.; Cerioni, G.; Plumitallo, A. *J. Org. Chem.* **1996**, 61, 3327.
- (3) Tardif, S. L.; Williams, C. R.; Harpp, D. N. *J. Am. Chem. Soc.* **1995**, 117, 9067.
- (4) Snyder, J. P.; Nevins, N.; Tardif, S. L.; Harpp, D. N. *J. Am. Chem. Soc.* **1997**, 119, 12685.
- (5) Schmidt, H.; Steudel, R.; Sülzle, D.; Schwarz, H. *Inorg. Chem.* **1992**, 31, 941.
- (6) Miaskiewicz, K.; Steudel, R. *J. Chem. Soc., Dalton Trans.* **1991**, 2395.
- (7) Gleiter, R.; Hyla-Kryspin, I.; Schmidt, H.; Steudel, R. *Chem. Ber.* **1993**, 126, 2363.
- (8) Koritsanszky, T.; Buschmann, J.; Luger, P.; Schmidt, H.; Steudel, R. *J. Phys. Chem.* **1994**, 98, 5416.
- (9) Steudel, R.; Schmidt, H.; Baumeister, E.; Oberhammer, H.; Koritsanszky, T. *J. Phys. Chem.* **1995**, 99, 8987.
- (10) Borghi, R.; Lunazzi, L.; Placucci, G.; Cerioni, G.; Foresti, E.; Plumitallo, A. *J. Org. Chem.* **1997**, 62, 4924.
- (11) Cerioni, G.; Cremonini, M. A.; Lunazzi, L.; Placucci, G.; Plumitallo, A. *J. Org. Chem.* **1998**, 63, 3933.
- (12) Tanaka, S.; Sugihara, Y.; Sakamoto, A.; Ishii, A.; Nakayama, J. *J. Am. Chem. Soc.* **2003**, 125, 9024.
- (13) Zysman-Colman, E.; Harpp, D. N. *J. Org. Chem.* **2005**, 70, 5964.
- (14) Zysman-Colman, E.; Nevins, N.; Eghbali, N.; Snyder, J. P.; Harpp, D. N. *J. Am. Chem. Soc.* **2006**, 128, 291.

- (15) Li, W. K.; Chiu, S. W.; Ma, Z. X.; Liao, C. L.; Ng, C. Y. *J. Chem. Phys.* **1993**, 99, 8440.
- (16) Snyder, J. P.; Carlsen, L. *J. Am. Chem. Soc.* **1977**, 99, 2931.
- (17) Erben, M. F.; Della Védova, C. O. *Inorg. Chem.* **2002**, 41, 3740.
- (18) Erben, M. F.; Della Védova, C. O. *Helv. Chim. Acta* **2003**, 86, 2379.
- (19) Palmar, K. J. *J. Am. Chem. Soc.* **1938**, 60, 2360.
- (20) Wang, C. S.; Pullen, K. E.; Shreeve, J. M. *Inorg. Chem.* **1970**, 9, 90.
- (21) Zeng, X. Q.; Liu, F. Y.; Sun, Q.; Ge, M. F.; Zhang, J. P.; Ai, X. C.; Meng, L. P.; Zheng, S. J.; Wang, D. X. *Inorg. Chem.* **2004**, 43, 4799.
- (22) Zeng, X. Q.; Ge, M. F.; Sun, Z.; Wang, D. X. *Inorg. Chem.* **2005**, 44, 9283.
- (23) Frisch, M. J.; Trucks, G. W.; Schlegel, H. B.; Scuseria, G. E.; Robb, M. A.; Cheeseman, J. R.; Zakrzewski, V. G.; Montgomery, J. A., Jr.; Stratmann, R. E.; Burant, J. C.; Dapprich, S.; Millam, J. M.; Daniels, A. D.; Kudin, K. N.; Strain, M. C.; Farkas, O.; Tomasi, J.; Barone, V.; Cossi, M.; Cammi, R.; Mennucci, B.; Pomelli, C.; Adamo, C.; Clifford, S.; Ochterski, J.; Petersson, G. A.; Ayala, P. Y.; Cui, Q.; Morokuma, K.; Malick, D. K.; Rabuck, A. D.; Raghavachari, K.; Foresman, J. B.; Cioslowski, J.; Ortiz, J. V.; Stefanov, B. B.; Liu, G.; Liashenko, A.; Piskorz, P.; Komaromi, I.; Gomperts, R.; Martin, R. L.; Fox, D. J.; Keith, T.; Al-Laham, M. A.; Peng, C. Y.; Nanayakkara, A.; Gonzalez, C.; Challacombe, M.; Gill, P. M. W.; Johnson, B. G.; Chen, W.; Wong, M. W.; Andres, J. L.; Head-Gordon, M.; Replogle, E. S.; Pople, J. A. *Gaussian 98*, revision A.5; Gaussian, Inc.: Pittsburgh, PA, 1998.
- (24) Becke, A. D. *J. Chem. Phys.* **1993**, 98, 5648.
- (25) Lee, C.; Yang, W.; Parr, R. G. *Phys. Rev. B* **1988**, 37, 785.
- (26) Niessen, Von W.; Schirmer, J.; Cederbaum, L. S. *Comput. Phys. Rep.* **1984**, 1, 57.
- (27) Ulic, S. E.; Della Védova, C. O.; Hermann, A.; Mack, H.-G.; Oberhammer, H. *Inorg. Chem.* **2002**, 41, 5699.
- (28) Priefer, R.; Lee, Y. J.; Barrios, F.; Wosnick, J. H.; Lebus, A.-M.; Farrell, P. G.; Harpp, D. N.; Sun, A.; Wu, S.; Snyder, J. P. *J. Am. Chem. Soc.* **2002**, 124, 5626.
- (29) Taha, A. N.; True, N. S. *J. Phys. Chem. A* **2000**, 104, 2985.
- (30) Laidig, K. E.; Cameron, L. M. *J. Am. Chem. Soc.* **1996**, 118, 1737.
- (31) Raban, M.; Yamamoto, G. *J. Am. Chem. Soc.* **1979**, 101, 5890.
- (32) Rablen, P. R.; Miller, D. A.; Bullock, V. R.; Hutchinson, P. H.; Gorman, J. A. *J. Am. Chem. Soc.* **1999**, 121, 218.
- (33) Rablen, P. R. *J. Org. Chem.* **2000**, 65, 7930.
- (34) Wiberg, K. B.; Breneman, C. M. *J. Am. Chem. Soc.* **1992**, 114, 831.
- (35) Yokozeki, A.; Bauer, S. H. *J. Phys. Chem.* **1976**, 80, 618.
- (36) Hermann, A.; Ulic, S. E.; Della Védova, C. O.; Mack, H.-G.; Oberhammer, H. *J. Fluorine Chem.* **2001**, 112, 297.
- (37) Erben, M. F.; Della Védova, C. O.; Willner, H.; Trautner, F.; Oberhammer, H.; Boese, R. *Inorg. Chem.* **2005**, 44, 7070.
- (38) Ulic, S. E.; von Ahsen, S.; Willner, H. *Inorg. Chem.* **2004**, 43, 5268.
- (39) Ulic, S. E.; Kosma, A.; Leibold, C.; Della Védova, C. O.; Willner, H.; Oberhammer, H. *J. Phys. Chem. A* **2005**, 109, 3739.
- (40) Redington, R. L.; Olson, W. B.; Cross, P. C. *J. Chem. Phys.* **1962**, 36, 1311.
- (41) Halpern, A. M.; Glendening, E. D. *J. Chem. Phys.* **2004**, 121, 273.
- (42) Hedberg, L.; Hedberg, K.; Eller, P. G.; Ryan, R. R. *Inorg. Chem.* **1988**, 27, 232.
- (43) Birk, M.; Friedl, R. R.; Cohen, E. A.; Pickett, H. M.; Sander, S. P. *J. Chem. Phys.* **1989**, 91, 6588.
- (44) Mack, H.-G.; Della Védova, C. O.; Oberhammer, H. *Angew. Chem., Int. Ed. Engl.* **1991**, 30, 1145.
- (45) Kopitzky, R.; Willner, H.; Hermann, A.; Oberhammer, H. *Inorg. Chem.* **2001**, 40, 2693.
- (46) Baker, A. D.; Brisk, M.; Gellender, M. *J. Electron Spectrosc. Relat. Phenom.* **1974**, 3, 227.
- (47) Boyd, D. B. *J. Am. Chem. Soc.* **1972**, 94, 8799.
- (48) Sweigart, D. A.; Turner, D. W. *J. Am. Chem. Soc.* **1972**, 94, 5592.